

# AGING STUDIES OF ATOMIC LAYER EPITAXY ZnS:Mn ALTERNATING-CURRENT THIN-FILM ELECTROLUMINESCENT DEVICES

Mustafa M. Abdalla AHMED, Doctoral Degree Programme (2)  
Dept. of Physics, FEEC, BUT  
E-mail: xahmed00@stud.feec.vutbr.cz

Supervised by: Prof. Pavel Tománek

## ABSTRACT

A study of the aging behavior of atomic layer epitaxy (ALE) ZnS:Mn alternating-current thin-film electroluminescent (ACTFEL) devices is undertaken by monitoring the internal charge-phosphor field ( $Q-F_p$ ) and capacitance-voltage ( $C-V$ ) characteristics as a function of aging time. The electrical properties are asymmetrical with respect to the applied voltage pulse polarity; the aging characteristics of such devices are also asymmetric.

## 1 INTRODUCTION

The aging characteristics and device stability of alternating-current thin-film electroluminescent (ACTFEL) flat-panel display devices have been the subject of numerous studies [1]. The majority of this work has focused on monitoring the luminescence of the ACTFEL device as a function of aging time. The purpose of the work discussed herein is to report an investigation of the aging properties of atomic layer epitaxy (ALE) ZnS:Mn ACTFEL devices. Instead of measuring the luminescent properties, we monitored the electrical properties of the ACTFEL devices as a function of aging time. Specifically, we assess the ACTFEL electrical properties using the capacitance-voltage ( $C-V$ ) [2] and internal charge-phosphor field ( $Q-F_p$ ) [3] techniques.

## 2 EXPERIMENTAL PROCEDURE

The ZnS:Mn ACTFEL devices are fabricated at Planar International by ALE in the typical stack configuration in which a 550 nm-thick ZnS:Mn layer is sandwiched between two layers of aluminum-titanium oxide (ATO) 270 nm thick which are contacted by a bottom indium tin oxide (ITO) and a top aluminum (Al) electrode. The area of the dots used in this study is  $0.0104 \text{ cm}^2$ .  $Q-F_p$  analysis is accomplished using the circuit shown in Fig. 1. An arbitrary waveform generator (Agilent 33220A) in conjunction with a high-voltage operational amplifier (7265 DSP) generates the small duty cycle bipolar pulse waveform which drives the series resistor,  $R_s=200 \text{ } \Omega$ , the ACTFEL device, and a sense capacitor,  $C_s=10$

nF. The driving waveform used is symmetric with alternating bipolar pulses of trapezoidal shape with 5 ps rise and fall times, a pulse width of 30  $\mu$ s, a maximum voltage amplitude of 210 V, and a frequency of 1 kHz; all of the data shown in this paper are obtained using this driving waveform. The  $Q$ - $F$  curve is generated by acquiring  $v_2(t)$  and  $v_3(t)$ , as indicated in fig. 1, using a digitizing oscilloscope (Agilent 54621A) and plotting the internal phosphor charge,  $q(t)$  versus the phosphor electrical field,  $F_p(t)$ , where

$$q(t) = \frac{c_i + c_p}{c_i} c_s v_3(t) - c_p [v_2(t) - v_3(t)] \quad (1)$$

( $C_i$  and  $C_p$  are the insulator and phosphor capacitances, respectively) and ( $d_p$  is the phosphor thickness).

$$F_p(t) = \frac{1}{d_p} \left( \frac{c_s v_3(t)}{c_i} - [v_2(t) - v_3(t)] \right) \quad (2)$$

$C$ - $V$  characteristics are obtained using the circuit shown in Fig. 1 except that the sense-capacitor is replaced by a current sense resistor,  $R_c = 7.6 \Omega$ . The  $C$ - $V$  curve is generated by plotting the dynamic capacitance as a function of the voltage across the ACTFEL device,  $C(v_2 - v_3)$ , given by

$$c(v_2 - v_3) = \frac{i(t)}{d[v_2(t) - v_3(t)]/dt} \quad (3)$$

versus the voltage across the ACTFEL device  $[v_2(t) - v_3(t)]$ . The current  $i(t)$  is obtained from the voltage across the current sense resistor,

$$i(t) = \frac{v_3(t)}{R_c} \quad (4)$$

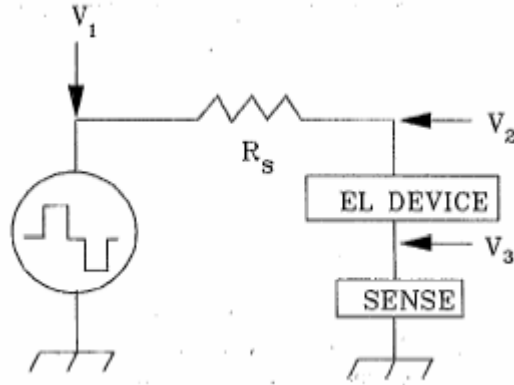


**Fig. 1:** Circuit used for ACTFEL electrical characterization

### 3 EXPERIMENTAL RESULTS

Figure 2 illustrates the  $C$ - $V$  characteristics as a function of aging time for a positive voltage pulse applied to the top Al electrode. Note that the  $C$ - $V$  curve shifts in a nonrigid manner with respect to aging time, this nonrigid shift in the  $C$ - $V$  curve indicates that the

interface state density in the preclamping regime,  $Q_{ss}$  increases as a function of aging time, as displayed quantitatively later. Moreover, notice how soft the  $C$ - $V$  curve becomes in the  $v_{to1}$  regime as aging continues; this softening indicates that electrons are injected from shallower interface states as aging progresses. Finally, note that the effective insulator capacitance  $C_i$  decreases with aging time, most of the decrease in  $C_i$  occurs during the initial 10h of aging.

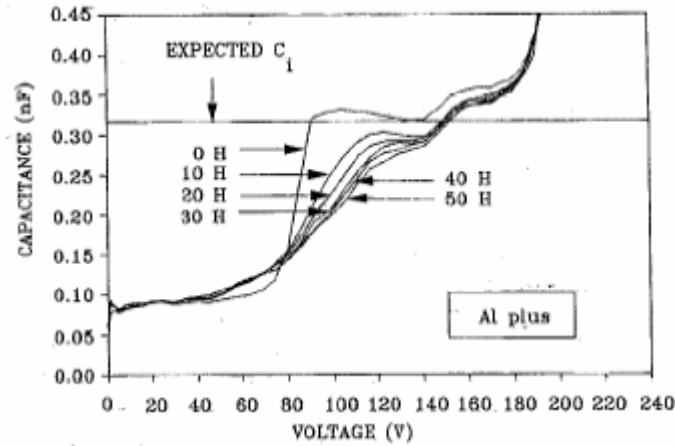


**Fig. 2:**  $C$ - $V$  curves as a function of aging time for an ALE ZnS:Mn ACTFEL device when the Al electrode is positively biased (i.e., emission from the ITO interface)

Figure 3 shows  $C$ - $V$  curves corresponding to various aging times for a negative voltage pulse applied to the top Al electrode.

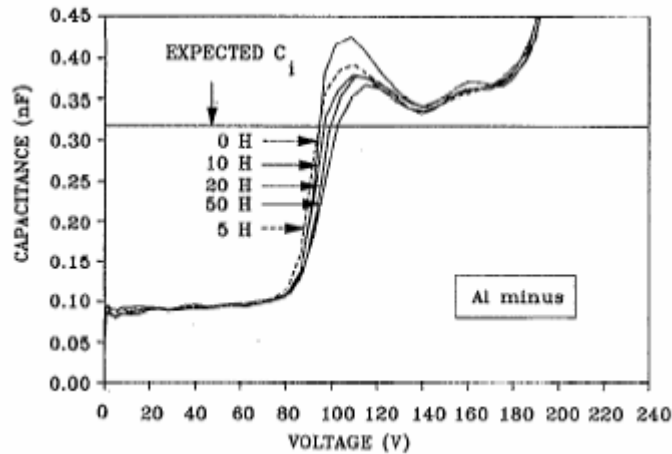


**Fig. 3:**  $C$ - $V$  curve as a function of aging time for an ALE ZnS:Mn ACTFEL device when the Al electrode is negatively biased (i.e., emission from the Al interface).

It is evident from a comparison of Figs. 2 and 3 that the  $C$ - $V$  curves corresponding to the two interfaces are quite different initially and that they display distinctly different aging trends. Hence, the electrical properties and aging characteristics of these interfaces are also quite different. The asymmetry trends we observe by  $C$ - $V$  analysis are similar to the conduction current-voltage curves reported by Mikami et al.[4]. Perhaps the most unusual aspect of the curves shown in Fig.3 is the  $C$ - $V$  overshoot which we interpret as evidence for

the buildup of space charge in the bulk ZnS phosphor. An overshoot in the  $Q$ - $F_p$  characteristics is also observed concomitant with  $C$ - $V$  overshoot; this is further evidence for space charge. Notice that the extent of the overshoot decreases with increasing aging time. Therefore, the amount of space charge which builds up in the ZnS decreases with aging. The second trend evident from Fig. 3 is that the  $C$ - $V$  curve first shifts rigidly to lower voltages and then shifts almost rigidly to higher voltages with increasing aging time. This rigid or almost rigid shift is interpreted as indicating that  $Q_{ss}$  is rather constant with aging. Furthermore, since these  $C$ - $V$  curves are rather steep,  $Q_{ss}$  is relatively small.

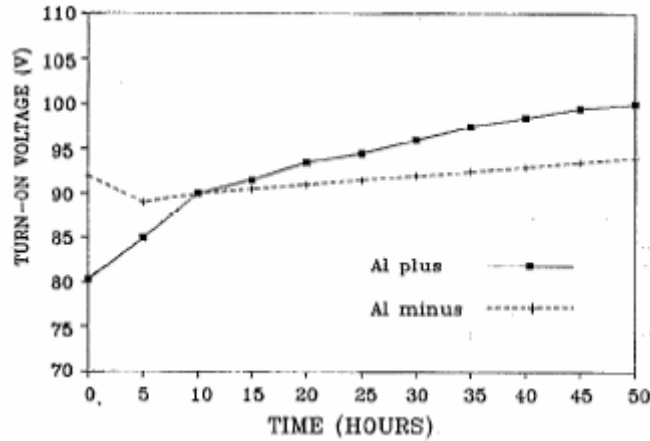


**Fig. 4:**  $v_{to2}$  vs aging time for an ALE ZnS:Mn ACTFEL device

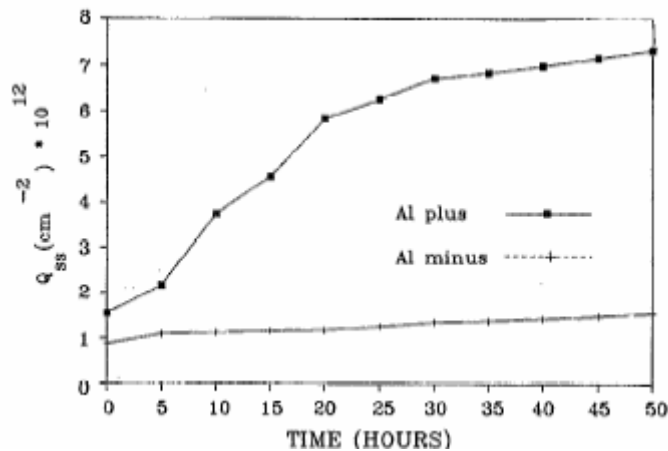


**Fig. 5:**  $Q_{ss}$  vs aging time for an ALE ZnS:Mn ACTFEL device.

Several of the  $C$ - $V$  trends discussed previously are summarized in Figs 4 and 5. Figure 4 is a plot of the turn-on voltage  $v_{to2}$ , as a function of aging time.  $v_{to2}$  for the bottom interface monotonically increases with aging time as the  $C$ - $V$  transition becomes broader.  $v_{to2}$  for the top interface first decreases slightly, then increases slowly, and finally saturates at a voltage similar to its original value. Figure 5 indicates the dramatic difference in the  $Q_{ss}$  aging trends for the two interfaces. Both interfaces exhibit an increase in  $Q_{ss}$  with aging time, but the change in the bottom interface is much larger.

## 4 CONCLUSION

An experimental study of the aging characteristics of ALE ZnS:Mn ACTFEL devices is presented in which aging is assessed by monitoring the electrical properties of these devices via C-V and Q-F, analysis. The electrical properties of these ALE devices are asymmetrical with respect to the polarity of the applied voltage pulse. This is in contrast to evaporated ZnS:Mn ACTFEL devices whose electrical and optical properties are quite symmetric. This asymmetry is in good agreement, however, with the results of previous workers. We attribute the experimentally observed asymmetry of the electrical properties to differences in the interface state densities of the top and bottom interfaces.

The most striking implication of the aging trends is that the interface state distributions at the top and bottom interfaces are asymmetric and, furthermore, exhibit highly asymmetric aging characteristics. This is clearly illustrated by the  $Q_{ss}$  aging trends shown in Fig. 5. In summary, our assessment of the experimental data shown in Figs. 2-5 leads to the following conclusions regarding the aging characteristics of ALE ZnS:Mn ACTFEL devices:

- 1) The interface state densities of the top and bottom interface are distinctly different and exhibit different aging characteristics.
- 2) Both shallow and deep traps are created during aging at the bottom interface.
- 3) A lesser number of predominately deep traps are created at the top interface during aging.
- 4) The decrease in  $C_i$  with aging indicates that some of the “interface state charge” actually moves deeper into the ZnS bulk with aging, and
- 5) The decrease in the C-V overshoot of the bottom interface indicates that the amount of space charge build up in the ZnS decreases with aging time.

## ACKNOWLEDGMENTS

This work was supported by the Czech Ministry of Education, Youth and Sport through a research plan MSM 262200022 MICROSYSY.

## REFERENCES

- [1] Inoguchi, T., Takeda, M., Kakihara, Y., Nakata, Y., Yoshida, M.: SID 74 Digest 5, p. 84–93, 1974